

Gradient pore size distributions in porous silicon oxycarbide materials

A. Tamayo^a, J. Rubio^{b,*}, R. Peña-Alonso^b, F. Rubio^b, J.L. Oteo^b

^a Department of Mechanical Engineering, Engineering Center–ECME Rm150, University of Colorado, Boulder, CO 80309-0427, USA

^b Instituto de Cerámica y Vidrio, CSIC, Campus Cantoblanco, C/ Kelsen, 5, 28049 Madrid, Spain

Received 29 July 2007; received in revised form 28 November 2007; accepted 16 December 2007

Available online 4 March 2008

Abstract

Hybrid materials have been obtained using a given concentration of tetraethylorthosilicate (TEOS) and polydimethylsiloxane (PDMS). Different size and shape monolithic samples have been achieved by using containers of both different evaporation areas and heights. The hybrid materials have been pyrolyzed under nitrogen atmosphere to yield porous silicon oxycarbide glasses, consisting of interconnected spherical particles and a continuous open-pore channel. The texture of the glasses shows a gradient particle size distribution (PtSD) from the top (2.88 μm) to the bottom (7.83 μm) of the samples. This gradient in the particle size leads also to a gradient distribution of porosities in the oxycarbide glasses. Thus, pore sizes increases from 6 μm at the top evaporation face to 13 μm at the bottom of the samples, and porosities in the corresponding regions decrease from 77% to 63%, respectively.

The gradient distribution has been assigned to a gradient concentration of PDMS in the hybrid preceramic material as determined by the elemental analysis. The carbon concentration (free and covalently bonded carbon) in the hybrid materials increases with the sample thickness or height. However, the lower concentration of PDMS molecules found at the bottom of the hybrid samples leads, after pyrolysis, to higher values of retained carbon and pore sizes in the SiOC glasses. An interesting finding is that the gradient PDMS distribution also provokes a gradient nanodomain size of the segregated free carbon as a form of graphite, typical in SiOC glasses.

© 2008 Elsevier Ltd. All rights reserved.

Keywords: Sol–gel process; SiOC; Gradient; Porosity; Evaporation

1. Introduction

The processing of silicon oxycarbide glasses through the pyrolysis of hybrid materials has been established as a novel route to prepare new advanced ceramics. Hybrid materials can be sol–gel processed by using silicon-modified alkoxides. Different silicon alkoxides such as TEOS (tetraethyl orthosilicate), TREOS (triethoxy silane), MTREOS (methyl triethoxysilane) or MDES (methyl diethoxy silane), can be used.^{1–3} Polysiloxanes, used themselves or mixed with silicon alkoxides may be also used as starting materials for obtaining SiOC glasses.^{4,5} In all cases, the hybrid material must be pyrolysed at about 1100 °C in inert atmosphere. During this pyrolytic process different reactions occur being those of redistribution and mineralization reactions the most important.^{1,6} Redistribution involves the exchange of Si–C/Si–O, Si–H/Si–O or Si–O/Si–O bonds. The

exchange of Si–H/Si–O bonds takes place at temperatures of about 300–400 °C and the exchange of Si–C/Si–O bonds occurs near 500–700 °C.⁷ At higher temperatures (800–1000 °C), mineralization reactions take place leading to the final inorganic material or SiOC glass. This silicon oxycarbide glass finally consists of Si–C and Si–O bonds whose chemical composition can be expressed as $\text{SiO}_x\text{C}_{4-x} + y\text{C}_{\text{free}}$, where $\text{SiO}_x\text{C}_{4-x}$ describes the composition of the “pure” silicon oxycarbide glass and $y\text{C}_{\text{free}}$ describes the presence of free carbon in the material.⁴

In general, redistribution reactions significantly modify the initial siloxane units of the hybrid material and lead to an escape of volatile silanes or siloxanes. On the other hand, mineralization reactions lead to the removal of methane and hydrogen from the material. In the low temperature range (300–700 °C) porosity is developed and an increase of the specific surface area is found. However, at higher temperatures (800–1100 °C) such porosity is reduced due to a shrinkage process and a reduction of the surface area is then observed. The development of such transient porosity during the pyrolysis process is a well known effect

* Corresponding author. Tel.: +34 91 735 58 55.
E-mail address: jrubio@icv.csic.es (J. Rubio).

observed for all the polymer-derived and hybrid-derived silicon oxycarbide glasses.^{6,8–10}


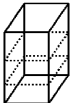


Porosity in silicon oxycarbide glasses has different effects according to their application. When high mechanical strength and chemical durability are needed, pore-free or dense silicon oxycarbide materials must be achieved.¹⁰ However, for high surface area silicon oxycarbide glasses, such as foams or catalytic supports, high porosities in both micro and mesopore ranges are needed.^{11,12} Different studies have demonstrated that silicon oxycarbide glasses have unique high temperature properties specially their mechanical strength and chemical durability.^{4,13} At the same time, it is also well known that pyrolysis conditions also have a strong effect on the reactions of converting the hybrid material into a silicon oxycarbide glass.^{14–16} Different relative amounts of silicon carbide, silicon oxide, and silicon oxycarbides can be developed depending on the structure of the starting hybrid material and the pyrolysis path. The porosity of these materials depends mainly on the type and network structure of the cross-linked hybrid precursor and on the conditions of pyrolysis, especially on the final temperature. The purpose of this work is to study the effect of the hybrid precursor size on the porosity of the final silicon oxycarbide glasses obtained.

Sol–gel-derived organically modified silicates (Ormosils) can be prepared from tetraethoxysilane (TEOS) and silanol terminated poly(dimethylsiloxane) (PDMS). These hybrid

materials have been pyrolysed in inert atmosphere at temperatures higher than 1000 °C to produce silicon oxycarbide glasses.^{5,17,18} The main advantage of these materials is the ease of producing bulk oxycarbide samples and their ability to develop a wide range of porous structures, depending on the synthesis conditions, catalyst type, amount of solvent, TEOS/PDMS molar ratio, chain length of polymer or type of reinforcing filler.^{16,19,20} It has also been found that for TEOS/PDMS pyrolysed materials their nanostructure-microhardness relationships are related to the variations of the average pore size.⁵ In such studies, it has been supposed that porosity is homogeneously distributed in the silicon oxycarbide glass. This hypothesis might be possible for low dimension samples even though it has been observed that pores are normally located in the core of the material.¹⁰

In this work, we have studied the distribution of pore sizes as a function of the sample dimension. Different shape and volume of SiOC monolithic samples, prepared from different height or thickness hybrid materials, have been obtained. The highest sample (approximately 76 mm) has been analyzed after being cut into slices (sample H) whereas the whole monolith has been analyzed for the rest of the samples (samples S, M and L). Material characterization was carried out by using mercury porosimetry, Raman spectroscopy, field-emission scanning electron microscopy (FE-SEM) and carbon content analysis.

Table 1
Geometric parameters of containers used for obtaining the SiOC glasses with different conformation: evaporation areas (mm²), volume filled (cm³) and sample height (mm, in parenthesis)

Container	Shape and dimension (length × depth × height)	Evaporation area (mm ²)	Filling volume, in cm ³ (SiOC thickness, in mm, height)	Sample name (SiOC glass) ^a
H	150 × 55 (height × diameter) 	24	150	H-7, H-42
			(76)	H-13, H-53 H-20, H-64 H-34, H-76
S	90 × 90 × 60 	81	100 (8)	S-8
			200 (20)	S-20
M	160 × 80 × 30 	128	100 (3)	M-3
			200 (8)	M-8
			300 (12)	M-12
L	240 × 90 × 50 	216	100 (2)	L-2
			200 (4)	L-4
			300 (7)	L-7
			600 (14)	L-14

^a The number attached to the letter identifying the conforming container and therefore, the shape of the SiOC glass denotes the thickness of the sample, except for sample H in which it accounts for the height at which every slice has been cut respect to the bottom of the sample.

2. Experimental procedure

2.1. Synthesis of hybrid materials and silicon oxycarbide glasses

Hybrid (preceramic) materials were obtained by sol–gel reaction between TEOS (Merck) and PDMS (1700 g mol^{-1} , ABCR) in a weight ratio of 60/40, H_2O , isopropanol (iPrOH, Merck) and HCl. The molar ratios $\text{H}_2\text{O}/\text{TEOS}$, HCl/TEOS and iPrOH/TEOS were 3, 0.3 and 6, respectively. A solution containing the H_2O , HCl and (1/2) iPrOH was rapidly added to the solution with $\text{TEOS}/\text{PDMS}/(1/2)\text{iPrOH}$. After 20 min of reflux, the sol was poured into plastic containers of different dimensions. The sol samples were gelled at room temperature in the closed containers (as it is shown in Table 1) and the exuded liquid was removed each 24 h. When no more liquid was exuded the resulting gels were dried at 50 and 100°C until no further weight loss was observed. The hybrid materials were pyrolyzed at 1100°C under flowing nitrogen ($150 \text{ cm}^3 \text{ min}^{-1}$) at a heating rate of 5°C min^{-1} and 2 h holding at the maximum temperature. Finally, the samples were cooled down to room temperature at $10^\circ\text{C min}^{-1}$. All pyrolyzed samples retained the shape of the hybrid monolith without evidence of crack development.

The solutions were gelled in four different containers, represented in Table 1 as H (high), S (small), M (medium) and L (large), to allow the evaluation of the effect of different evaporation surface areas on the porosity of the final SiOC samples. The occurrence of a compositional gradient from the core to the surface of the sample was studied by means of the length/section ratio for specimen). On the other hand, the effect of the different volume/surface ratio of the materials was studied by different volume filling of the containers S, M and L. As it will be discussed along the text, both heights (i.e. thickness) and evaporation surface areas are factors that determine the pore diameter and porosity of silicon oxycarbide glasses.

Table 1 reports on the different samples prepared in terms of evaporation area and volume of sol poured into the containers, as well as the thickness or height obtained for each corresponding SiOC glass. Obviously, higher filling volumes of solution result in higher (or thicker) SiOC samples. Analogously, the same volume of solution filling different type of container results in different thickness of SiOC material. Thus, samples S-8, M-3 and L-2 are produced from the same amount of solution but bigger surface container, this is, with bigger evaporation areas, respectively, and therefore the thickness of the samples decreases from S to L.

Thus, as pointed out in Table 1, type H specimens refers to those samples on a cylindrical container with 24 mm^2 of evaporation area filled with 150 cm^3 of solution. The 76 mm height SiOC monolith was cut in near 7 mm slices, distant from the bottom of the specimen, the number of mm indicated in the label. Container S (81 mm^2 of evaporation area) was filled with 2 different volume of solution (100 and 200 cm^3) which yield two SiOC materials of 8 and 20 mm thick, respectively. Similarly, three and four specimens of M and L type containers, respectively, were produced by increasing volumes of solution filling the containers.

Bulk SiOC glass materials from containers S, M and L were studied as obtained, whereas the individual discs were analyzed for type H specimen. In all cases the analyzed material was taken from the center of each sample.

2.2. Sample characterization

Hybrid and silicon oxycarbide materials were characterized by microstructural, structural and textural techniques. The microstructural analysis was carried out using a field emission scanning electron microscope (FE-SEM, Hitachi 4700) operating at 20 keV. Pore size distributions (PSDs) of the silicon oxycarbide glasses were determined by means of mercury porosimetry, using an Autopore II 9215 (Micromeritics Corp.). The maximum hydraulic pressure applied was 200 MPa. All samples were previously degassed at room temperature in order to remove any adsorbed liquid in the sample porosity. The total carbon content of the pyrolyzed materials was determined using an elemental analyzer (LECO Model CS-200). It must be emphasized that the total carbon content corresponds to the sum of both free and covalently bonded carbon existing in the silicon oxycarbide glasses. Finally, Raman spectroscopy was carried out by a Renishaw inVia spectrophotometer with a 514 nm wavelength laser. Raman spectra were obtained from the average of 10 scans from 100 to 3500 cm^{-1} using silicon as calibration source.

3. Results

3.1. Raman spectroscopy

Raman spectra of all prepared SiOC show two peaks characteristic of containing carbon materials.³ These bands, located around 1340 cm^{-1} (D band) and 1600 cm^{-1} (G band) correspond to disordered or defects ($\text{C}_{\text{sp}}^2\text{--C}_{\text{sp}}^3$ stretching mode) and ordered ($\text{C}_{\text{sp}}^2\text{--C}_{\text{sp}}^2$ bonds) graphite structures and allows the characterization of the size of the graphite nanodomain existing in the SiOC structure as it will be shown below.²¹

The spectra reported in Fig. 1 denote the high symmetry of both D and G peaks with a slightly higher intensity of the D peak respect to the G one for the S, M and L samples. However, for the H oxycarbide glasses it is observed that the intensities of the D and G bands are a function of the sample slice, i.e. the height at which the sample has been cut respect to the evaporation face. Thus, for low and medium height samples, H-7 to H-42, the D band is the highest, as it occurs in Fig. 1(a). However, for samples whose height is more than 42 mm the G band is more intense than the D one. This result evidences the structural changes that take place in the samples according to the distance to the evaporation face.

3.2. FE-SEM

The microstructure of the SiOC glasses has been studied through the analysis of the fracture surface by FE-SEM, as it is shown in Fig. 2. In order to use the same criteria for all samples, the FE-SEM analysis has been carried out always on

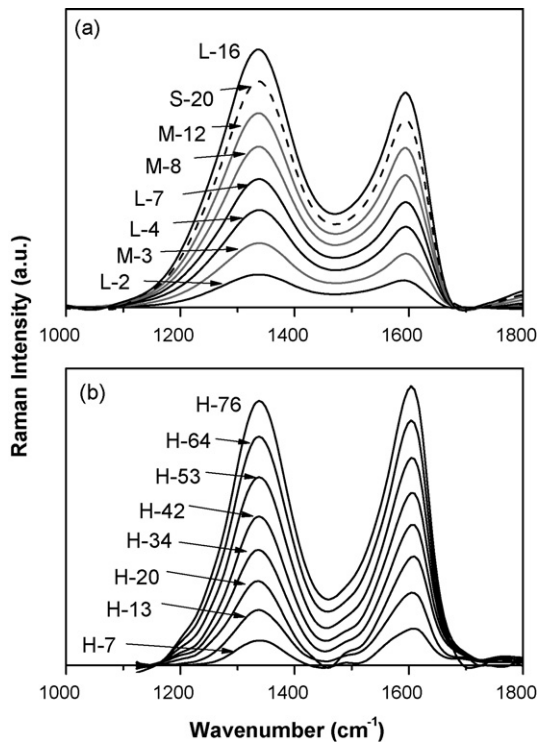


Fig. 1. Raman spectra of SiOC glasses: (a) specimens from S, M and L containers and (b) slice specimens from container H.

the center of each fractured sample. The porous microstructure of SiOC glasses is made of large aggregated spherical particles which form a continuous material. Porosity is due to the interstices that exist between the particles. The same

microstructure has been also observed for most hybrid materials synthesized from the TEOS–PDMS system through the sol–gel process^{17,22,23} and, as well for their derivatives SiOC materials.^{5,18} In this Fig. 2, a slightly bigger particle size is observed for the samples with the lower height. This result is associated here to the presence of different concentrations of PDMS on the bottom or top of the samples, as it will be further discuss in next sections. Since the initial PDMS concentration was the same for all the materials, such different PDMS concentration between the top and the bottom surfaces or between different thickness specimens must be due to an asymmetric or gradient distribution of PDMS molecules during the gelling of the specimen as it was already observed in silica-polysiloxane hybrid materials.²⁴

A further analysis of the gradient pore microstructure was developed by the study of the particle size distributions (PtSD). Thus, for each sample at least 220 particles were studied by an image analyzer, assuming spherical form. Fig. 3 shows the PtSD of each SiOC glass. The different plots evidence the strong dependence of the particle size with the height or thickness of the samples. The plots evidence the decrease of the particle size with the increase of the sample volume. In the case of sample H the decrease of the particle size is also directly related to the proximity of the slice to the evaporation face, thus, the biggest pores are found in the bottom slice and they decrease in dimension with the proximity to the evaporation face. For specimens types S, M and L, those samples thinner than 10 mm exhibit a bimodal PtSD with an average particle size in the range between 6 and 9 μm . However, thicker samples present a similar particle size of about 3.7 μm for all type of samples. Thus, the increase of the thickness of the preceramic hybrid results in a

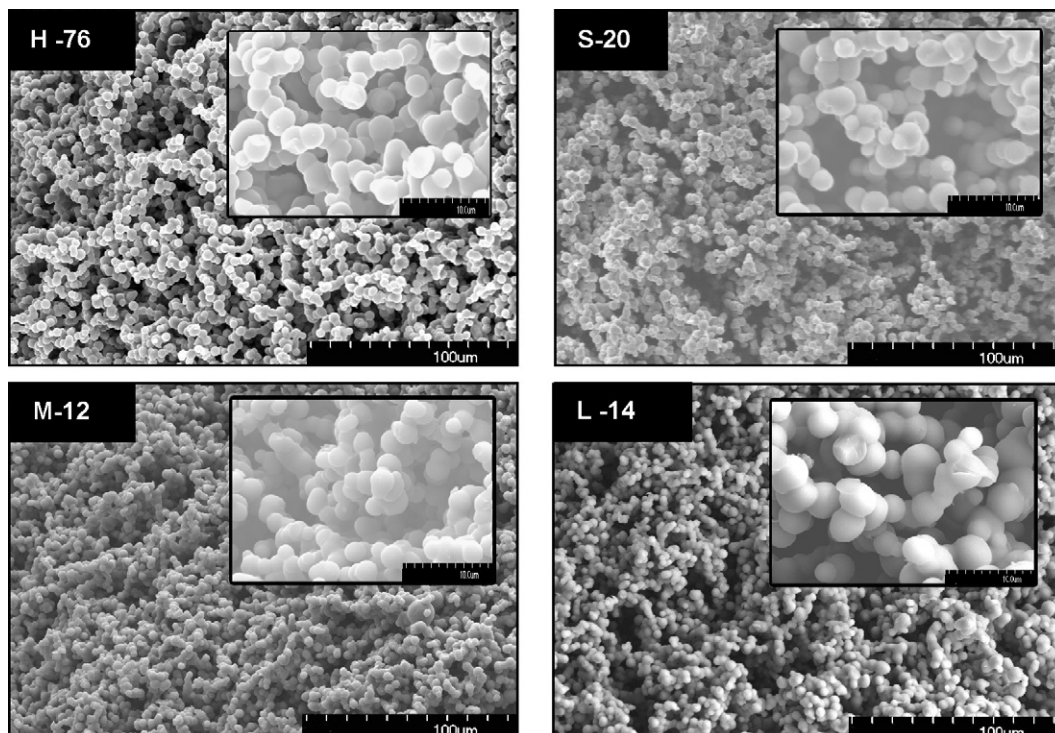


Fig. 2. FE-SEM micrographs for thick or higher heights SiOC glasses. Space bar for inside micrographs is 10 μm .

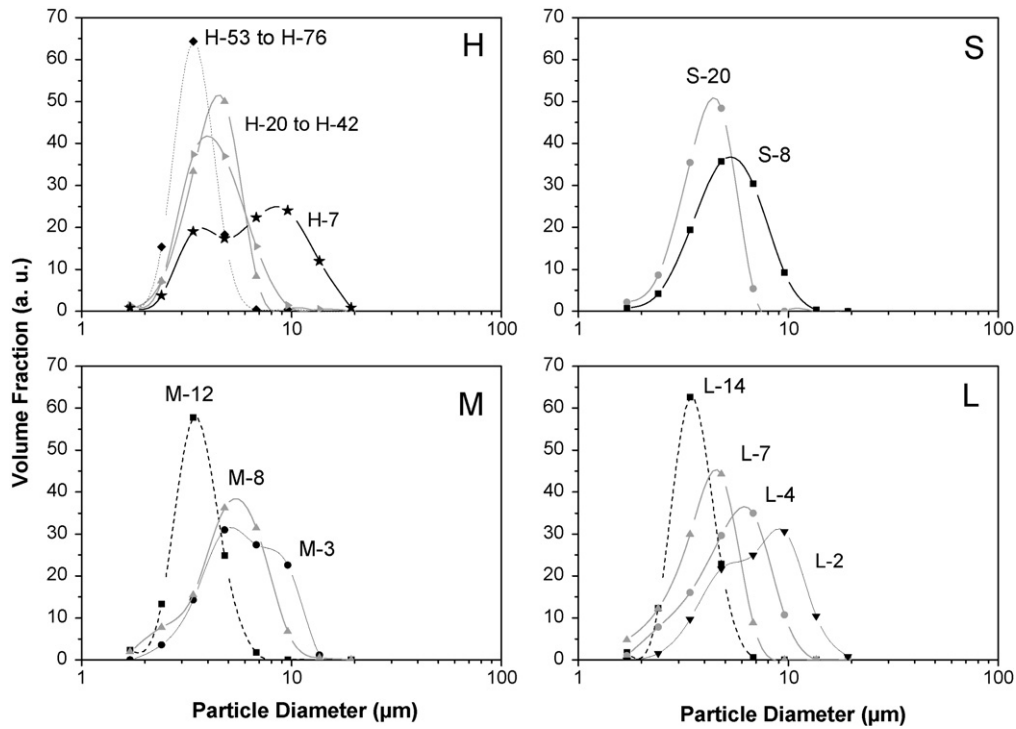


Fig. 3. Particle size distributions (PtSD) of the different height (sample H) and thickness (samples S, M and L) SiOC glasses.

decrease of the particle size in the oxycarbide materials. This result shows the remarkable fact of an asymmetrical or, better, a gradient pore size and porosity distributions through the sample, as a function of the distance of the aggregates to the evaporation surface.

3.3. Pore size distributions (PSDs)

Accordingly to the findings of last section, Fig. 4 shows the differential pore volume of the SiOC materials as a function of their pore diameter. PSDs of samples H are upward shifted with

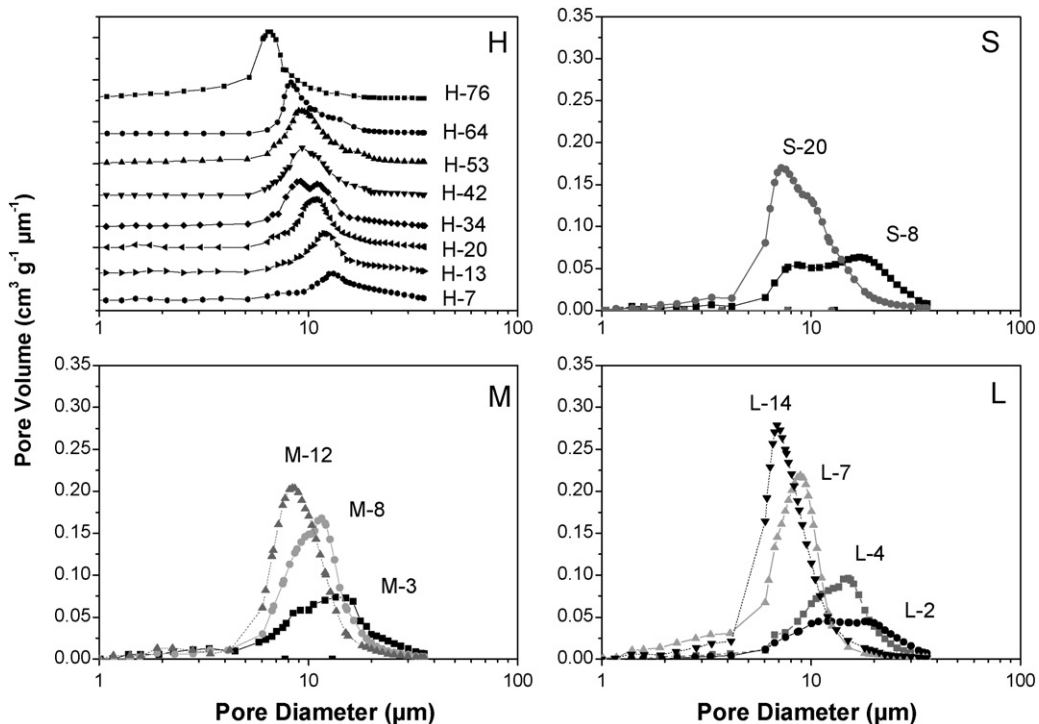


Fig. 4. Pore size distributions (PSD) of different height and thickness SiOC glasses.

the only purpose of offering a clearer view. The general trend for SiOC glasses prepared in containers S, M and L exhibits a broad PSD with pores between 5 and 30 μm for samples thinner than 10–12 mm. However, when the samples are thicker than 12 mm both narrower PSDs and smaller pores appear. Therefore, the pore size decreases with the increase of the filling volume independently on the shape of the container. On the other hand, the PSDs corresponding to specimens H, show that the gradient distribution of pore sizes is also found within the same sample if it is sufficiently high. Analogously to the behaviours of specimens S, M and L, the narrowest distributions of pores and smallest pore sizes in sample H are found in the slice at the evaporation face (top sample, H-76) and much wider PSDs and greater mean pore size are exhibited at the bottom (H-7).

These results are in accordance with the SiOC particle size observed in the micrographs from Fig. 2. In summary, thicker (i.e. higher) samples possess both smaller particles and pore sizes than those of thinner specimens.

4. Discussion

The above results have shown that gradient functional distributions of both particle and pore sizes are found in silicon oxycarbide samples if their longitudinal dimensions (thickness or heights) are sufficient. This conclusion has also been found by Chevalier et al.²⁴ for thin layers of porous hybrid TEOS-polysiloxane materials. However, they found a different microstructure only at the bottom and top of the layer suggesting that the bottom was enriched in silica and the top in polysiloxane. At the same time, they observed a denser (non-porous) layer close to the top surface, which agrees our finding of smaller pore dimensions on the evaporation slice (Fig. 4). The asymmetrical polysiloxane distribution leads to gradient pore sizes and surface areas in the hybrid materials and, therefore, in their corresponding pyrolyzed materials, the silicon oxycarbide glasses.

Fig. 5a represents the mean pore size for all the studied samples. The linear fitting of every set of data leads to the same value of the intercept around 14 μm for the mean pore diameter, independently of their different conformation parameters. Thus, a SiOC glass, made from the same TEOS/PDMS composition, with a low thickness (i.e. a thick coating or thick film) would have a maximum pore size of about 14 μm . However, the increase of thickness results in a decrease of pore size, showing a minimum value of 6 μm for the thicker specimen. On the other hand, the decrease of the evaporation area results in a decrease of the fitting slope, and therefore in a decrease of the gradient. This result must be related to the syneresis process during gelling of the preceramic hybrid. Therefore, the highest evaporation face is translated in a faster syneresis. This process leads to a more rapid removal of alcohol, H_2O and non-bonded PDMS molecules and, consequently to a lower gelling time, that finally is reflected in a higher variation of the pore diameter.

On the other hand, Fig. 5b shows the porosity of the studied oxycarbide materials. Thinner specimens show a porosity value close to 63%, which increases with the sample thickness, up to 20 mm, where porosity reaches 77%. Specimens thicker

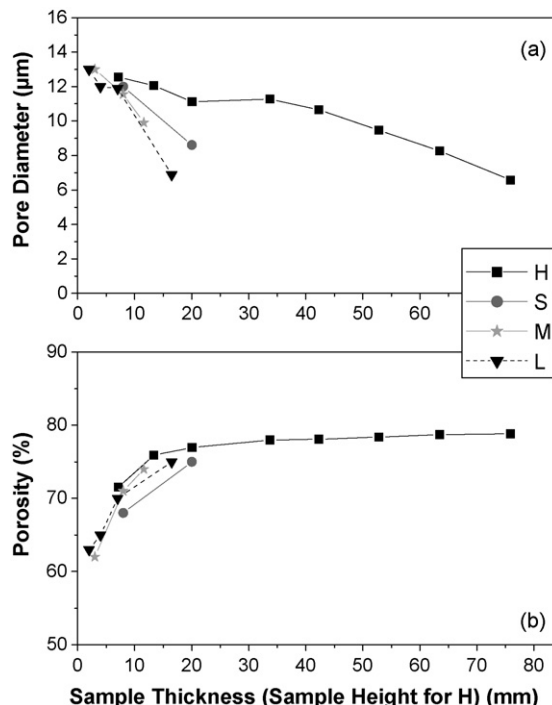


Fig. 5. Evolution of (a) average pore size and (b) porosity in SiOC glasses.

than 20 mm asymptotically approach 80% of porosity. The same change occurred at a sample thickness close to 20 mm is also observed in the PSDs of Fig. 5a. On the other hand, it is important to notice and remark that the dimension of the evaporation area has a minimum influence on the porosity of the silicon oxycarbide glasses, as it is shown in Fig. 5b.

The observed behaviour of the PSDs, pore sizes and porosities of SiOC glasses of different thickness must be related to the silica/polymer distribution in the core of the corresponding hybrid samples during the gelling occurrence. Mackenzie and co-workers observed a wide distribution of porosities and PSDs when changing HCl/TEOS , PDMS/TEOS and $\text{H}_2\text{O}/\text{TEOS}$ ratios in TEOS–PDMS hybrid materials.^{17,25,26} In their works they used ^{29}Si NMR spectroscopy and assigned the observed microstructures to different velocities of self-condensation of TEOS and/or polycondensation TEOS–PDMS reactions. Guo et al.²³ also observed these microstructures and analyzed the nanometer and micrometer scales of the hybrid materials by using SAXS and SEM. The nanometer scaled showed a crossover from compact structures (primary particles) to mass-fractals, with the primary particles close to 3 nm, while the mass-fractals decreased from 10 to 5 nm with the increase of the PDMS concentration. Nevertheless, such increase of PDMS did not modify the primary particle size and mass-fractal aggregate sizes, but only produced an increase of the pore size observed by SEM.

In our work, the determination of a gradient PDMS concentration in the obtained hybrids was evaluated through the carbon analysis in both, hybrid and glass materials (Fig. 6). As far as the carbon of the samples is only due to PDMS, the results exposed in Fig. 7 point out the inhomogeneous distribution of PDMS in the whole hybrid monolith. The gradient concentration of PDMS

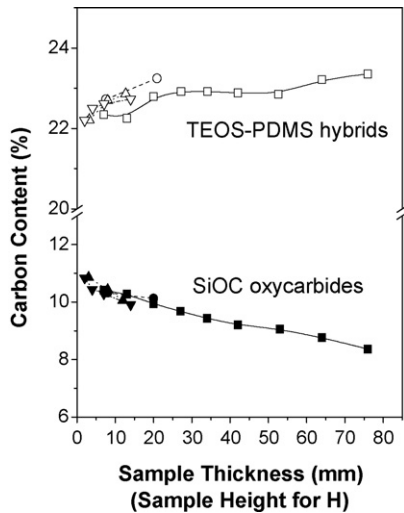


Fig. 6. Carbon content on preceramic hybrids and SiOC glasses.

in the hybrid samples is also dependent on the thickness and evaporation area of each specimen. Fig. 6 shows that for a given hybrid sample height, the carbon concentration increases in the order $H < S < M < L$, i.e. which correspond to the order of the evaporation areas of the samples. This result indicates that the removal of non-bonded PDMS molecules or cyclic polysiloxanes is easier for samples with higher evaporation surface areas. Therefore, both shape and size of the hybrid leads to specific concentrations of carbon in the material and hence to specific pore sizes.

The results of Fig. 6 also evidence the higher amount of carbon, i.e. more PDMS molecules, in thicker specimens. This enrichment in elastomer on the top surface of hybrid materials is similar to that reported by Chevalier et al.²⁴ by studies of material fracture. Chevalier found that the surface has a thin layer of dense (non-porous) material, which varies considerably from place to place within the sample. The explanation proposed by Guo et al.²³ assumed a great extension of the polycondensation reaction between PDMS and TEOS (hydrolyzed) molecules. Thus, the higher PDMS concentration produces a higher polyconden-

sation which finally results in a lower pore size, as it is shown in Fig. 5a. Chevalier et al.²⁴ described also the film bottom face as consisting only in silicon and oxygen atoms with no traces of carbon. In our studies, the presence of carbon founded also in the thinnest specimens is due to the fact of having monolithic samples of 2 mm of minimum thickness, while as the data from Chevalier refers to thin membranes (layer).

On the other hand, the carbon content of the SiOC glasses (Fig. 6) follows the opposite trend as the preceramic hybrids. The samples exhibit a continuous decrease of the carbon content of the silicon oxycarbide glasses from the bottom surface to the top of the sample. A similar result has been obtained by Rouxel et al.²⁷ who found a decrease of the carbon content of silicon oxycarbide glasses from the surface to the center of the sample, and that such decrease appeared also when different oxycarbide precursors are used. Now, in this work, the carbon content fall on the same line for all the specimens and depends only on the sample thickness but not on the evaporation surface area. This result indicates that the carbon concentration remaining in the silicon oxycarbide glass is directly related to the PDMS/TEOS ratio, as Sorarù proposed.² The question arises to the understanding why a higher concentration of carbon in the preceramic material leads to a lower concentration in the SiOC glass? Since the thickest preceramic samples exhibit higher carbon content and lower pore sizes, analogous data would be expected in the corresponding SiOC glasses as the low pore size would restrict the diffusion of PDMS molecules to escape from the material. However, the founded results behave the opposite. The analysis of this fact has its bases in the Raman spectra presented in Fig. 1.

According to Knight and White, from Raman spectra of graphite like materials one could derive the in-plane crystallite size of the graphitic nanodomains, L_a , from the relative intensities of the D (1310 cm^{-1}) and G (1600 cm^{-1}) bands following the formula²⁸:

$$L_a(\text{nm}) = 4.4 \left(\frac{I_G}{I_D} \right)$$

The evolution trend of the L_a values obtained from the gaussian deconvolution of the presented Raman spectra is shown in Fig. 7. Graphite nanodomain sizes in the range between 2.04 and 2.45 nm are found for the SiOC glasses from S, M, L containers. Nanodomain size for the type H glasses are founded to be between 2.33 and 6.35 nm. Thus, the graphite nanodomain continuously increases with the increase of the sample thickness.

This result together with those deduced from Figs. 5a and 6 concludes the gradient distribution of PDMS in the preceramic materials according to their higher molecular weights. According to Rouxel et al.²⁷ the carbon heterogeneous distribution is due to the processing of the samples. Such gradient distribution is not so noticeable in thin monoliths as a major amount of PDMS molecules can be dragged along with solvent during drying process. Nevertheless, the PDMS rich regions provoke the appearance of high pore diameters in the pyrolyzed materials. We postulate that, during pyrolysis, the TEOS molecules surrounding the PDMS favour the carbon retention in the pyrolyzed materials. Thus, thin SiOC samples exhibits higher carbon content and lower graphite nanodomains due to the smaller abun-

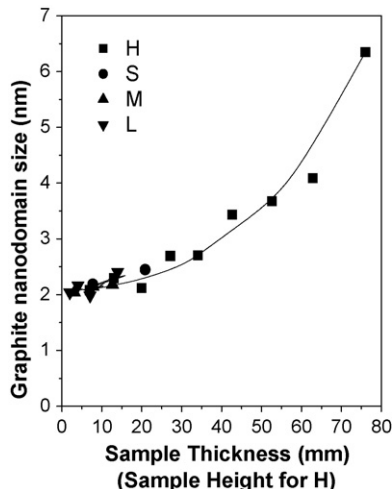


Fig. 7. Graphite nanodomain sizes of SiOC glasses.

dance of PDMS. Moreover, a gradient on the PDMS molecular weight would induce the appearance of pores possessing a size directly related to it. In that way, redistribution reactions, faster for PDMS of low molecular weight, would produce a further growing of the graphite nanodomains. However, the more PDMS concentration in the preceramic material, the higher the graphite nanodomain sizes.

In summary, the obtained silicon oxycarbide glasses present a gradient of both, pore sizes and carbon concentration, from the bottom to the top sides of the sample and this carbon gradient does not depend either on the size of the container nor on their evaporation area. This heterogeneous distribution of carbon gives also a gradient on the graphite nanodomain sizes which present the opposite trend: as the carbon content decreases the graphite nanodomain increases. Accordingly to Rouxel et al.²⁷ the increase of the carbon content results in an increase of free-carbon content, and, consequently, the turbostratic graphite domains. The presence of a higher carbon content is responsible for the more normal indentation patterns observed by Rouxel et al.²⁷ for float glass as well as silicon oxycarbide glasses. This behaviour is suggested to be due to the covalently bonded carbon atoms which decrease the mobility of the residual vitreous silica network at the molecular scale. However, another suggestion can be made in accordance with the size of the graphite nanodomains, which can act as network modifiers like sodium and calcium in float glass giving the above mentioned normal indentation behaviour. As the carbon content decreases the graphite nanodomain increases and they may be separated from the glass structure as a new phase reach in carbon where the whole phase would be a high reach silica phase (such as vitreous silica) with its corresponding anomalous indentation behaviour.

5. Conclusions

This work has pointed out that SiOC materials prepared from monolithic hybrids of PDMS and TEOS exhibit a gradient distributions of porosity, particle size, carbon content and graphite nanodomain size. These gradient distributions have been assigned to a gradient concentration of PDMS in the hybrid or preceramic material. The higher concentration of PDMS molecules is found at the top of the preceramic material and leads to lower pore sizes in the pyrolyzed silicon oxycarbide glasses.

The obtained silicon oxycarbide glasses consist of interconnected spherical particles where a continuous open-pore channel structure is formed. It has been found that the sample particle size increases from 2.88 to 7.83 μm by increasing the distance from the evaporation surface in thick samples (approximately 76 mm). However, thinner and, at the same time, higher evaporation surface area samples present values for the particle size in the range between 2.97 and 6.15 mm.

For thick samples, the pore size decreases from 13 to 6 μm and porosity increases from 63% to 77%, with the increase of the sample thickness. However, even though pore size continuously decreases with the increase of the sample thickness, porosity values asymptotically approach 80% for samples thicker than 15–30 mm. At such dimension the PSDs of the SiOC glass shows

a bimodal pore distribution with well-separated pores of 9 and 11 μm . The final pore size of the silicon oxycarbide glass is indirectly dependent on the evaporation surface area of the confining container, thus, as the evaporation area increases, the pore size decreases. This conclusion is related to the PDMS distribution in the hybrids. On the other hand, it has been found that porosity is mainly dependent of the container but not on the evaporation surface.

The presence of a gradient distribution on PDMS molecules led also to different graphite nanodomain sizes of the free carbon and the SiOC glasses exhibited a gradient nanodomain size distribution. The nanodomain size of graphite increases with the thickness of the sample from 2.04 to 6.35 nm.

Acknowledgements

This work was supported by the Ministerio de Educación y Ciencia of Spain by the Project Ref. CTQ2006-15692-C02-02, and by the Comunidad de Madrid by the Project Ref. S-0505/PPQ/000344. R. Peña-Alonso is grateful to the Ministerio de Educación y Ciencia from Spain for financial support under post-doctoral fellowship resol. 27-04-05. A. Tamayo is grateful to the University of Colorado at Boulder for financial support under post-doctoral grant.

References

1. Belot, V., Corriu, R. J. P., Leclercq, D., Mutin, P. H. and Vioux, A., Thermal reactions occurring during pyrolysis of crosslinked polysiloxane gels, precursors to silicon oxycarbide glasses. *J. Non-Cryst. Solids*, 1992, **147/148**, 52–55.
2. Sorarù, G. D., Silicon oxycarbide glasses from gels. *J. Sol-gel Sci. Technol.*, 1994, **2**, 843–848.
3. Pantano, C. G., Singh, A. K. and Zhang, H., Silicon oxycarbide glasses. *J. Sol-gel Sci. Technol.*, 1999, **14**, 7–25.
4. Sorarù, G. D., Modena, S., Guadagnino, E., Colombo, P., Egan, J. and Pantano, C., Chemical durability of silicon oxycarbide glasses. *J. Am. Ceram. Soc.*, 2002, **85**(2), 1529–1536.
5. Flores, A., Martos, C., Sánchez-Cortés, S., Rubio, F., Rubio, J. and Oteo, J. L., Nanostructure and micromechanical properties of silica/silicon oxycarbide porous composites. *J. Am. Ceram. Soc.*, 2004, **87**(11), 2093–2100.
6. Greil, P., Active-filler-controlled pyrolysis of preceramic polymers. *J. Am. Ceram. Soc.*, 1995, **78**(4), 835–848.
7. Belot, V., Corriu, R. J. P., Leclercq, D., Mutin, P. H. and Vioux, A., Thermal redistribution reactions in crosslinked polysiloxanes. *J. Polym. Sci. A: Polym. Chem.*, 1992, **30**(4), 613–623.
8. Wynne, K. J. and Rice, R. W., Ceramics by polymer pyrolysis. *Ann. Rev. Mater. Sci.*, 1984, **14**, 297–334.
9. Riedel, R., Advances ceramics from inorganic polymers. In *Materials Science and Technology, A Comprehensive Treatment, Vol 17B, Processing of Ceramics, Part II*, ed. R. J. Brook. VCH, Wurzburg, 1996, pp. 1–50.
10. Walter, S., Sorarù, G. D., Brequel, H. and Enzo, S., Microstructural and mechanical characterization of sol gel-derived Si–O–C glasses. *J. Eur. Ceram. Soc.*, 2002, **22**, 2389–2400.
11. Liu, D., Zhang, H., Komarneni, S. and Pantano, G. C., Porous silicon oxycarbide glasses from organically modified silica gels of high surface area. *J. Sol-gel Sci. Technol.*, 1994, **1**, 141–151.
12. Toury, B. and Babonneau, F., Synthesis of periodic mesoporous organosilica from bis(triethoxysilyl)methane and their pyrolytic conversion into porous SiOC glasses. *J. Eur. Ceram. Soc.*, 2005, **25**, 265–270.
13. Rouxel, T., Massouras, G. and Sorarù, G. D., High temperature behavior of a gel-derived SiOC glass: elasticity and viscosity. *J. Sol-gel Sci. Technol.*, 1999, **14**, 87–94.

14. Hurwitz, F. I., Heimann, P., Farmer, S. C. and Hembree, D. M., Characterization of the pyrolytic conversion of polysilsesquioxanes to silicon oxycarbides. *J. Mater. Sci.*, 1993, **28**, 6622–6630.
15. Hurwitz, F. I., Heimann, P. J. and Kacik, T. A., Redistribution reactions in Blackglas™ during pyrolysis and their effect on oxidative stability. *Ceram. Eng. Sci. Proc.*, 1995, **16**(4), 217–224.
16. Peña-Alonso, R., Rubio, F., Rubio, J. and Oteo, J. L., Characterisation of the pyrolysis process of boron-containing ormosils by FT-IR analysis. *J. Anal. Appl. Pyrol.*, 2004, **71**, 827–845.
17. Mackenzie, J. D., Chung, Y. J. and Hu, Y., Rubbery ormosils and their applications. *J. Non-Cryst. Solids*, 1992, **147/148**, 271–279.
18. Martos, C., Rubio, F., Rubio, J. and Oteo, J. L., Infiltration of SiO₂/SiOC nanocomposites by a multiple sol infiltration-pyrolysis process. *J. Sol-gel Sci. Technol.*, 2003, **26**, 511–516.
19. Martos, C., Rubio, F., Rubio, J. and Oteo, J. L., Characterization of the pyrolysis process and structure of silicon oxycarbide based materials from organically modified silicate gels. *Key Eng. Mater.*, 2004, **264–268**, 351–354.
20. Peña-Alonso, R., Rubio, F., Rubio, J. and Oteo, J. L., Effect of pyrolysis temperature on the texture of ormoborosil materials for obtaining SiBOC oxycarbide glasses. *Key Eng. Mater.*, 2004, **264–268**, 1847–1850.
21. Gouadec, G., Colomban, P. and Bansal, N. P., Raman study of Hi-Nicalon-fiber-reinforced celsian composites: I. Distribution and nanostructure of different phases. *J. Am. Ceram. Soc.*, 2001, **84**(5), 1129–1135.
22. Huang, H. H., Orlor, G. and Wilkes, G. L., Ceramers—hybrid materials incorporating polymeric oligomeric species with inorganic glasses by a sol-gel process. 2. Effect of acid content on the final properties. *Polym. Bull.*, 1985, **14**(6), 557–564.
23. Guo, L., Hyeon-Lee, J. and Beaucage, G., Structural analysis of poly(dimethylsiloxane) modified silica xerogels. *J. Non-Cryst. Solids*, 1999, **243**, 61–69.
24. Chevalier, Y., Grillet, A.-C., Rahmi, M.-I., Liere, C., Masure, M., Hemery, P. et al., The structure of porous silica-polysiloxane hybrid materials. *Mater. Sci. Eng. C*, 2002, **21**, 143–150.
25. Chung, Y. J., Ting, S.-J. and Mackenzie, J. D., Rubbery ormosils. *Mater. Res. Soc. Symp. Proc.*, 1990, **180**, 961–996.
26. Iwamoto, T., Morita, K. and Mackenzie, J. D., Liquid state ²⁹Si NMR study on the sol-gel reaction mechanisms of ormosils. *J. Non-Cryst. Solids*, 1993, **159**, 65–72.
27. Rouxel, T., Sangleboeuf, J.-C., Guin, J.-P., Keryvin, V. and Sorarù, G.-D., Surface damage resistance of gel-derived oxycarbide glasses: hardness, toughness, and scratchability. *J. Am. Ceram. Soc.*, 2001, **84**(10), 2220–2224.
28. Dresselhaus, M. S., Pimenta, M. A., Eklund, P. C. and Dresselhaus, G., Raman scattering in fullerenes and related carbon-based materials. In *Raman Scattering in Materials Science*, ed. W. H. Weber and R. Merlin. Springer, Berlin, Germany, 2000 [Chapter 8].